Journal Pre-proof

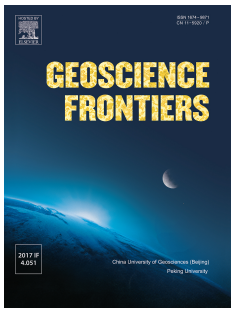

Aluminum solubility in bridgmanite up to 3000 K at the top lower mantle

Zhaodong Liu, Ran Liu, Yuchen Shang, Fangrui Shen, Luyao Chen, Xuyuan Hou, Mingguang Yao, Tian Cui, Bingbing Liu, Tomoo Katsura

PII: S1674-9871(20)30111-0

DOI: https://doi.org/10.1016/j.gsf.2020.04.009

Reference: GSF 996

To appear in: *Geoscience Frontiers*

Received Date: 21 October 2019

Revised Date: 1 February 2020

Accepted Date: 12 April 2020

Please cite this article as: Liu, Z., Liu, R., Shang, Y., Shen, F., Chen, L., Hou, X., Yao, M., Cui, T., Liu, B., Katsura, T., Aluminum solubility in bridgmanite up to 3000 K at the top lower mantle, *Geoscience Frontiers*, https://doi.org/10.1016/j.gsf.2020.04.009.

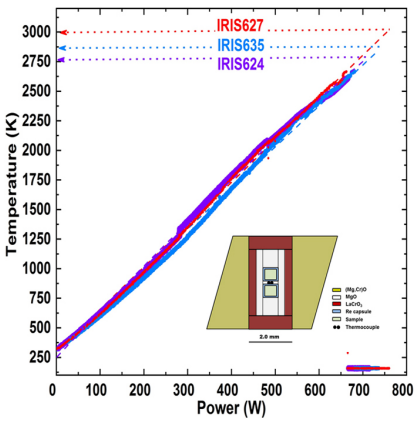

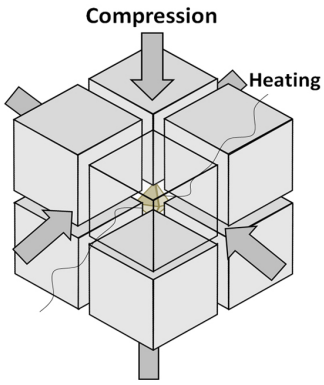

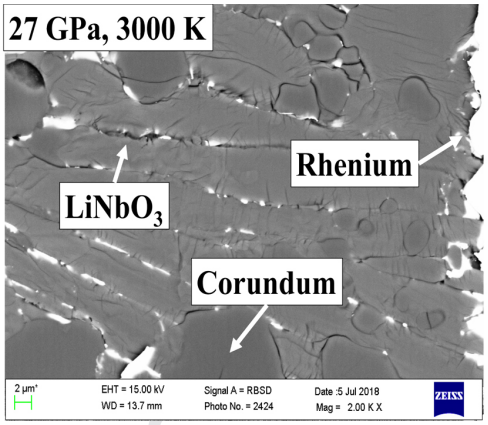

Aluminum solubility in bridgmanite up to 3000 K at the top lower mantle

Zhaodong Liu[a, b,*], Ran Liu[b], Yuchen Shang[b], Fangrui Shen[b], Luyao Chen[b], Xuyuan, Hou[b], Mingguang Yao[b], Tian Cui[b], Bingbing Liu[b], Tomoo Katsura[a,c]

[a] *Bayerisches Geoinstitut, University of Bayreuth, Bayreuth 95440, Germany*

[b] *State Key Laboratory of Superhard Materials, Jilin University, Changchun 130012, China*

[c] *Center for High Pressure Science and Technology Advanced Research, Beijing 100094, China*

* Corresponding author. E-mail address: liu_zhaodong@jlu.edu.cn (Zhaodong Liu)

Abstract

The temperature dependence of the Al_2O_3 solubility in bridgmanite has been determined in the system $MgSiO_3$–Al_2O_3 at temperatures of 2750–3000 K under a constant pressure of 27 GPa using a multi-anvil apparatus. Bridgmanite becomes more aluminous with increasing temperatures. A $LiNbO_3$-type phase with a pyrope composition ($Mg_3Al_2Si_3O_{12}$) forms at 2850 K, which is regarded as to be transformed from bridgmanite upon decompression. This phase contains 30 mol% Al_2O_3 at 3000 K. The $MgSiO_3$ solubility in corundum also increases with temperatures, reaching 52 mol% at 3000 K. Molar volumes of the hypothetical Al_2O_3 bridgmanite and $MgSiO_3$ corundum are constrained to be 25.95 ± 0.05 and 26.24 ± 0.06 cm^3/mol, respectively, and interaction parameters of non-ideality for these two phases are 5.6 ± 0.5 and 2.2 ± 0.5 KJ/mol, respectively. The increases in Al_2O_3 and $MgSiO_3$ contents, respectively, in bridgmanite and corundum are caused by a larger entropy of Al_2O_3 bridgmanite plus $MgSiO_3$ corundum than that of $MgSiO_3$ bridgmanite plus Al_2O_3 corundum with temperature, in addition to the configuration entropy. Our study may help explain dynamics of the top lower mantle and constrain pressure and temperature conditions of shocked meteorites.

Keywords: Bridgmanite; $LiNbO_3$-type phase; Corundum; Temperature; Entropy; Lower mantle

1. Introduction

Geochemical and petrological studies suggest that Earth's lower mantle (660–2900 km depth), which occupies more than 50% of Earth's volume, is the largest geochemical reservoir in the Earth (e.g., Ringwood, 1975; Anderson, 1983; McDonough and Sun, 1995). Bridgmanite is the most abundant phase in this region, and comprises about 80% of this region in volume (Irifune, 1994). Under lower-mantle conditions, bridgmanite can contain 25 mol% of alumina (Al_2O_3) (Liu et al., 2016, 2017a), which is far beyond its contents in the pyrolite and mid-oceanic ridge basalt (MORB) compositions (Green et al., 1979; Sun, 1982). Bridgmanite is thus the major host phase for the Al_2O_3 in the lower mantle (Irifune, 1996; Liu et al., 2016, 2017a). Al_2O_3 incorporation can greatly change chemical and physical properties of bridgmanite (e.g., McCammon, 1997; Xu et al., 1998; Zhang and Weidner, 1999; Brodholt, 2000). Therefore, the Al_2O_3 solubility in bridgmanite is of great significance for understanding the mineralogy of the lower mantle.

The Al_2O_3 solubility in bridgmanite has been studied in the system $MgSiO_3$–Al_2O_3 by several workers (Irifune et al., 1996; Kubo and Akaogi, 2000; Hirose et al., 2001; Akaogi et al., 2002). Liu et al. (2017a, 2017b) recently demonstrated that the Al_2O_3 solubility in bridgmanite has both positive pressure and temperature dependences at pressures of 27–52 GPa and temperatures of 1700–2500 K. They also predicted that a $LiNbO_3$-structured phase (LN) with a pyrope ($Mg_3Al_2Si_3O_{12}$) composition should form at 2750–2800 K under 27 GPa upon decompression. LN has been regarded as a metastable phase formed from high-pressure stable bridgmanite by a diffusionless transformation upon decompression (e.g., Ross et al., 1989; Liu et al., 2006). The formation of LN can help understand the complicated crystal chemistry of bridgmanite and constrains shock conditions of meteorites (Ishii et al., 2017; Liu et al., 2019). However, the temperature dependence of Al_2O_3 solubility in bridgmanite is still poorly understood because the data obtained by our recent (Liu et al., 2017b) and earlier (Irifune et al., 1996; Kubo and Akaogi, 2000; Hirose et al., 2001; Akaogi et al., 2002) studies did not agree well. Furthermore, the chemistry of Al_2O_3 component in bridgmanite remains unknown at temperatures higher than 2500 K. At higher

temperatures, oxygen vacancies in the form of an $MgAlO_{2.5}$ component should increase, and might thereby decrease the Al_2O_3 component (Brodholt, 2000; Navrotsky et al., 2003; Liu et al., 2019a, 2019b), which should decrease ferropericlase in the lower mantle. Temperatures in hot plumes from the lower mantle should be significantly higher by 500–1000 K than the surrounding mantle (e.g., Farnetani, 1997). Consequently, temperature effects are vital to constrain dynamics of the lower mantle. Nevertheless, our limited knowledge about the Al_2O_3 solubility in bridgmanite at very high temperatures prevents our understandings mantle dynamics.

Here, we investigated the Al_2O_3 solubility in bridgmanite at temperatures up to 3000 K and a constant pressure of 27 GPa in a multi-anvil press. This pressure can prevent the formation of majoritic garnet. Based on our new results, we have determined the temperature dependence of the Al_2O_3 solubility in bridgmanite together with the $MgSiO_3$ solubility in corundum, estimated thermoelastic parameters of bridgmanite and corundum, and discussed their implications for dynamics of the lower mantle.

2. Experimental methods

$En_{75}Cor_{25}$ ($Mg_3Al_2Si_3O_{12}$, En: $MgSiO_3$, Cor: Al_2O_3; the number represents mol%) and $En_{65}Cor_{35}$ glasses are used as starting materials. Detailed chemical composition of the $En_{75}Cor_{25}$ glass was reported in Liu et al. (2016), and that of the $En_{65}Cor_{35}$ glass was confirmed in the present study to have the intended composition using an electron probe microanalyzer. Starting materials were put into rhenium (Re) capsules made of 25 µm thick foils, and then heated at 500 K for half an hour to purge water. The capsules with starting materials were finally put into cell assemblies. Quench experiments at a constant pressure of 27 GPa and temperatures of 2700–3000 K were performed using a Cr_2O_3-doped MgO (OMCR, Mino Ceramic Co., LTD.) octahedra with a 7-mm edge length and $LaCrO_3$ sleeves for heating in combination with tungsten carbide cubes with 3 mm truncated edge lengths in a multi-anvil apparatus (IRIS-15) with a press load of 15 MN at the Bayerisches Geoinstitut, University of Bayreuth (Ishii et al., 2016). Temperature was monitored with a $W_{97}Re_3$-$W_{75}Re_{25}$

thermocouple placed adjacent to the Re capsule. The adapted cell assembly can be referred to Fig. 1. The pressure at high temperatures was calibrated by the decomposition of pyrope into aluminous bridgmanite and corundum and the Al_2O_3 solubility in bridgmanite at various temperatures (Liu et al., 2017b). Pressure uncertainties of these quench experiments are ± 1 GPa.

Phases in quench runs were identified using a micro-focused X-ray diffractometer (XRD, Bruker, D8 DISCOVER) equipped with a Co tube operated at 40 kV and 500 μA. X-ray beams were focused to 50 μm in diameter using an IFG polycapillary X-ray mini-lens. The XRD profile of each sample was collected for three hours. Textural observation was performed using a LEO1530 scanning electron microscope (SEM) operating at an acceleration voltage of 15 kV and a beam current of 10 nA. Chemical compositions of each phase present in the quench runs were determined using a JEOL JXA-8200 electron probe microanalyzer (EPMA) operating at acceleration voltages of 15 kV and a beam current of 5 nA with standards of enstatite for Mg and Si, and corundum for Al.

3. Results

Experimental conditions and phases present in the recovered samples are listed in Table 1.

Fig. 1a shows cross section of the cell assembly, and Fig. 1b plots the generated temperature as a function of the power supplied by the $LaCrO_3$ heater at 27 GPa. It is clearly seen that the temperature can successfully read 2399 °C. Above this temperature, we cannot read temperature because it exceeded the limit of temperature display of the thermometer. We thereby estimated the temperature from the extrapolation by a cubic polynomial fitting of the temperatures below 2399 °C and heating power. In the run 627, the heating power reached ~760 W and the estimated temperature was ~3000 ± 50 K.

Fig. 2 shows the XRD patterns of run products. Fig. 3 shows their back-scattered electron (BSE) images. At 2750 K, both XRD and BSE observations exhibit that run products from $En_{75}Cor_{25}$ consist of LN with trace amounts of corundum, bridgmanite,

and stishovite (Figs. 2a and 3a). We assume that LN is a product of back-transformation of bridgmanite upon decompression based on previous results (Funamori et al., 1997; Miyajima et al., 1999; Liu et al., 2016, 2017a; Ishii et al., 2017). Therefore, we refer to the composition of LN as "bridgmanite composition" hereafter. The formation of large amounts of LN in this bulk composition indicates that bridgmanite incorporates close to 25 mol% of Al_2O_3 even at the pressure much lower than previous studies, above 40 GPa (Liu et al., 2017). Trace amounts of bridgmanite may be a metastable remnant from the back-transition. The BSE image shows no distinguishable BSE signal intensities between LN and bridgmanite, indicating identical compositions of these two phases. One of these phases (bridgmanite) should therefore be metastable based on no binary phase loop of these two phases. From the run at 2850 K, the run product completely consists of a single LN with grain sizes larger than 10 μm. From the runs at 2850 and 3000 K from $En_{65}Cor_{35}$, the run product consists of a mixture of LN and corundum based on XRD identifications and BSE observations (Figs. 2c, d and 3c, d).

One question is whether melting occurs at the highest experimental temperature of 3000 K (run 627). SEM observations, however, did not show any features of melting in this run as follows. First, phase compositions are identical within analytical uncertainties in the radial direction. Second, although particles of Re or its oxide are found in the boundary of LN and corundum (Fig. 3b–d), the amounts of these particles significantly increase from the center to the ends of the sample capsule. These Re phases are thought to have been formed by a solid diffusion of the capsule at very high temperatures (Thévenin et al., 1993). Furthermore, Kudo and Ito (1996) studied the melting phase relations in this system at 25 GPa and reported that bridgmanite with 10 mol% Al_2O_3 melted at higher temperature than the melting temperature of the pure $MgSiO_3$ bridgmanite, which is 2900 K. Their report suggested that the incorporation of Al_2O_3 component must raise the melting temperature of bridgmanite. These observations and report lead to the conclusion that melting did not occur at the temperature of the run 627. Therefore, the melting temperature of bridgmanite with the $En_{75}Cor_{25}$ composition should be higher than 3000 K at 27 GPa.

Compositional analysis by EPMA confirms that LN/bridgmanite contained 24 ± 1 mol% Al_2O_3 at 2750 K from the $En_{75}Cor_{25}$ starting material. The LN in the run 635 from this starting material contained 25.0 ± 0.2 mol% Al_2O_3 at 2850 K, which is identical to that of the starting material. From the $En_{65}Cor_{35}$ starting material in the same run, the Al_2O_3 content in LN reached 26 ± 1 mol%, while the $MgSiO_3$ content in corundum was 42 ± 1 mol%. In the run 627 (3000 K), the Al_2O_3 content in LN and the $MgSiO_3$ content in corundum were found to be 29 ± 1 and 52 ± 1 mol%, respectively. The lattice parameters of this LN (a = b = 4.849 (1) Å; c = 12.712 (10) Å; the number in the parenthesis represents the standard deviation for the last digit.) are slightly higher than obtained by Ishii et al. (2017) those (a = b = 4.783 (2) Å; c = 12.680 (11) Å). These differences can be explained by the higher Al_2O_3 content in the present study. As already mentioned, the formation of these Al-rich LN was recovered from bridgmanite synthesized at lower-mantle conditions through a diffusionless transition, in which the A (Mg) cations are substituted and BO_6 (B, Si) octahedra are distorted due to the incorporation of large amounts of Al (Liu et al., 2016, 2019; Ishii et al., 2017).

4. Discussion

4.1. Thermodynamics of Al partitioning in bridgmanite and corundum

To further understand the Al^{3+} exchange between bridgmanite and corundum, we conducted the thermodynamics calculation using the following reaction:

$$MgSiO_3\ (Brg) + Al_2O_3\ (Cor) = Al_2O_3\ (Brg) + MgSiO_3\ (Cor) \quad (1)$$

where Al_2O_3 and $MgSiO_3$ are the hypothetical end-member of bridgmanite (Brg) and corundum (Cor), respectively. The Gibbs free energy change of reaction (1) can be expressed as:

$$\mu^{\mathrm{Brg}}_{\mathrm{MgSiO_3}} + \mu^{\mathrm{Cor}}_{\mathrm{Al_2O_3}} = \mu^{\mathrm{Brg}}_{\mathrm{Al_2O_3}} + \mu^{\mathrm{Cor}}_{\mathrm{MgSiO_3}} \quad (2)$$

where $\mu^{\mathrm{Brg}}_{\mathrm{MgSiO_3}}$ and $\mu^{\mathrm{Brg}}_{\mathrm{Al_2O_3}}$ are the chemical potentials of $MgSiO_3$ and Al_2O_3 in bridgmanite, respectively, and $\mu^{\mathrm{Cor}}_{\mathrm{Al_2O_3}}$ and $\mu^{\mathrm{Cor}}_{\mathrm{MgSiO_3}}$ are those of Al_2O_3 and $MgSiO_3$

components in corundum, respectively. Chemical potentials of these components can be expressed as the following equations in the non-ideal solution model:

$$\mu^{\mathrm{Brg}}_{\mathrm{MgSiO_3}} = \mu^{\circ\mathrm{Brg}}_{\mathrm{MgSiO_3}} + RT\ln a^{\mathrm{Brg}}_{\mathrm{MgSiO_3}} \quad (3)$$

$$\mu^{\mathrm{Cor}}_{\mathrm{Al_2O_3}} = \mu^{\circ\mathrm{Cor}}_{\mathrm{Al_2O_3}} + RT\ln a^{\mathrm{Cor}}_{\mathrm{Al_2O_3}} \quad (4)$$

$$\mu^{\mathrm{Brg}}_{\mathrm{Al_2O_3}} = \mu^{\circ\mathrm{Brg}}_{\mathrm{Al_2O_3}} + RT\ln a^{\mathrm{Brg}}_{\mathrm{Al_2O_3}} \quad (5)$$

$$\mu^{\mathrm{Cor}}_{(\mathrm{Mg_{0.5}Si_{0.5}})_2\mathrm{O_3}} = \mu^{\circ\mathrm{Cor}}_{\mathrm{MgSiO_3}} + RT\ln a^{\mathrm{Cor}}_{\mathrm{MgSiO_3}} \quad (6)$$

where $\mu^{\circ\mathrm{Brg}}_{\mathrm{MgSiO_3}}$, $\mu^{\circ\mathrm{Cor}}_{\mathrm{Al_2O_3}}$, $\mu^{\circ\mathrm{Brg}}_{\mathrm{Al_2O_3}}$, and $\mu^{\circ\mathrm{Cor}}_{(\mathrm{Mg_{0.5}Si_{0.5}})_2\mathrm{O_3}}$ are the standard chemical potentials of the (hypothetical) endmembers of these four components, and $a^{\mathrm{Brg}}_{\mathrm{MgSiO_3}}$, $a^{\mathrm{Cor}}_{\mathrm{Al_2O_3}}$, $a^{\mathrm{Brg}}_{\mathrm{Al_2O_3}}$, and $a^{\mathrm{Cor}}_{\mathrm{MgSiO_3}}$ are their activities. At equilibrium, the standard state Gibbs free energy change of reaction (1) can be then expressed as:

$$\Delta G^0_{R1} = \mu^{\circ\mathrm{Brg}}_{\mathrm{Al_2O_3}} + \mu^{\circ\mathrm{Cor}}_{(\mathrm{Mg_{0.5}Si_{0.5}})_2\mathrm{O_3}} - \mu^{\circ\mathrm{Brg}}_{\mathrm{MgSiO_3}} - \mu^{\circ\mathrm{Cor}}_{\mathrm{Al_2O_3}} = RT\ln a^{\mathrm{Brg}}_{\mathrm{MgSiO_3}} + RT\ln a^{\mathrm{Cor}}_{\mathrm{Al_2O_3}} - RT\ln a^{\mathrm{Brg}}_{\mathrm{Al_2O_3}} - RT\ln a^{\mathrm{Cor}}_{\mathrm{MgSiO_3}} \quad (7)$$

The activity coefficients for these components in bridgmanite and corundum can be expressed as:

$$a^{\mathrm{Brg}}_{\mathrm{Al_2O_3}} = (X^{\mathrm{Brg}}_{\mathrm{Al_2O_3}} \cdot \gamma^{\mathrm{Brg}}_{\mathrm{Al_2O_3}})^2 \quad (8)$$

$$a^{\mathrm{Brg}}_{\mathrm{MgSiO_3}} = (X^{\mathrm{Brg}}_{\mathrm{MgSiO_3}} \cdot \gamma^{\mathrm{Brg}}_{\mathrm{MgSiO_3}})^2 \quad (9)$$

$$a^{\mathrm{Cor}}_{\mathrm{Al_2O_3}} = (X^{\mathrm{Cor}}_{\mathrm{Al_2O_3}} \cdot \gamma^{\mathrm{Cor}}_{\mathrm{Al_2O_3}})^2 \quad (10)$$

$$a^{\mathrm{Cor}}_{\mathrm{MgSiO_3}} = (X^{\mathrm{Cor}}_{\mathrm{MgSiO_3}} \cdot \gamma^{\mathrm{Cor}}_{\mathrm{MgSiO_3}})^2 \quad (11)$$

By assuming the symmetric solutions for bridgmanite and corundum, their activity coefficients can be written as:

$$RT\ln\gamma^{\mathrm{Brg}}_{\mathrm{Al_2O_3}} = W^{\mathrm{Brg}}_{\mathrm{Al}}(1 - X^{\mathrm{Brg}}_{\mathrm{Al_2O_3}})^2 \quad (12)$$

$$RT\ln\gamma^{\mathrm{Brg}}_{\mathrm{MgSiO_3}} = W^{\mathrm{Brg}}_{\mathrm{Al}}(1 - X^{\mathrm{Brg}}_{\mathrm{MgSiO_3}})^2 \quad (13)$$

$$RT\ln\gamma^{\mathrm{Cor}}_{\mathrm{Al_2O_3}} = W^{\mathrm{Cor}}_{\mathrm{Al}}(1 - X^{\mathrm{Cor}}_{\mathrm{Al_2O_3}})^2 \quad (14)$$

$$RT\ln\gamma^{\mathrm{Cor}}_{\mathrm{MgSiO_3}} = W^{\mathrm{Cor}}_{\mathrm{Al}}(1 - X^{\mathrm{Cor}}_{\mathrm{MgSiO_3}})^2 \quad (15)$$

where $X^{\mathrm{Brg}}_{\mathrm{Al_2O_3}}$ and $X^{\mathrm{Brg}}_{\mathrm{MgSiO_3}}$ are the mole fractions of Al_2O_3 and $MgSiO_3$ in bridgmanite, respectively, $X^{\mathrm{Cor}}_{\mathrm{Al_2O_3}}$ and $X^{\mathrm{Cor}}_{\mathrm{MgSiO_3}}$ are the mole fractions of Al_2O_3 and $MgSiO_3$ components in the corundum, respectively, and $W^{\mathrm{Brg}}_{\mathrm{Al}}$ and $W^{\mathrm{Cor}}_{\mathrm{Al}}$ are the interaction parameters of bridgmanite and corundum of the symmetric solutions, respectively. ΔG^0_{R1} can be expressed as:

$$\Delta G^0_{\mathrm{R1}} = -2RT\ln\frac{X^{\mathrm{Cor}}_{\mathrm{MgSiO_3}}X^{\mathrm{Brg}}_{\mathrm{Al_2O_3}}}{X^{\mathrm{Cor}}_{\mathrm{Al_2O_3}}X^{\mathrm{Brg}}_{\mathrm{MgSiO_3}}} + 2W^{\mathrm{Cor}}_{\mathrm{Al}}\left(1-2X^{\mathrm{Cor}}_{\mathrm{Al_2O_3}}\right) + 2W^{\mathrm{Brg}}_{\mathrm{Al}}\left(2X^{\mathrm{Brg}}_{\mathrm{Al_2O_3}}-1\right) \quad (16)$$

Molar volumes of bridgmanite and corundum as a function of the Al_2O_3 and $MgSiO_3$ contents, respectively, are summarized in Fig. 4 (D′Amour et al., 1978; Ito et al., 1978; Irifune et al., 1996; Kubo and Akaogi, 2000; Liu et al., 2016, 2017a). It is clearly seen that molar volumes of bridgmanite and corundum, respectively, increase almost linearly with increasing Al_2O_3 and $MgSiO_3$ contents within analytical uncertainties. A linear relation leads to the following equation for the bridgmanite volume in cm^3/mol:

$$V_{\mathrm{Brg}} = 24.44 + 0.0151(5)\times \chi_{\mathrm{Al2O3}} \quad (17)$$

where χ_{Al2O3} represents the mole fraction of the Al_2O_3 in bridgmanite. The derived molar volume of the hypothetical Al_2O_3 bridgmanite is to be 25.95 ± 0.05 cm^3/mol. Since the molar volume of corundum is 25.56 cm^3/mol under ambient conditions (D′Amour et al., 1978), the volume of Al_2O_3 bridgmanite is larger than that of pure corundum.

The same equation for corundum produces the following equation in cm^3/mol:

$$V_{\mathrm{Cor}} = 25.56 + 0.0068\ (6)\times\chi_{\mathrm{MgSiO3}} \quad (18)$$

where χ_{MgSiO3} represents mole fractions of the $MgSiO_3$ content in corundum. It is thus found that the effect of $MgSiO_3$ contents on the volume of corundum is significantly smaller than that of Al_2O_3 for bridgmanite. We have derived the molar volume of the hypothetical $MgSiO_3$ corundum of 26.24 ± 0.06 cm^3/mol. This value is very close to the volume of $MgSiO_3$ akimotoite, which is 26.35 cm^3/mol (Horiuchi et al., 1982). Since akimotoite has an ilmenite-structure, which is a modification of the corundum structure by cation ordering, the $MgSiO_3$-bearing corundum may form a continuous

232 solid solution with akimotoite, and cation ordering may occur from a certain
233 composition in the Al_2O_3–$MgSiO_3$ system (Panero et al., 2003).

234 We derive $W_{\mathrm{Al}}^{\mathrm{Cor}}$ and $W_{\mathrm{Al}}^{\mathrm{Brg}}$ by an empirical method for the non-ideality of solid
235 solutions due to a mismatch of the component volumes using the following formula
236 (Davies and Navrotsky, 1983; Akaogi and Ito, 1999):

237 $$W_{\mathrm{G}} = 100.8\Delta V - 0.4 \text{ kJ/mol} \quad (19)$$

238 $$\Delta V = \frac{V_A - V_B}{(V_A + V_B)/2} \quad (20)$$

239 where V_{A} and V_{B} are the molar volumes of the larger and smaller components,
240 respectively. We then obtained the $W_{\mathrm{Al}}^{\mathrm{Brg}}$ and $W_{\mathrm{Al}}^{\mathrm{Cor}}$ values of 5.6 ± 0.2 and 2.2 ± 0.2
241 kJ/mol, respectively, from the present molar volume results and equations of (17) and
242 (18).

243 In Fig. 5, the derived ΔG_{R1}^0 from reaction (16) changes from 106 ± 13 kJ·mol^{-1}
244 at 1700 K to 75 ± 7 kJ·mol^{-1} at 2300 K and to 38 ± 4 kJ·mol^{-1} at 3000 K. The
245 composition data of bridgmanite and corundum at temperatures of 1700–2500 K is
246 from Liu et al. (2016, 2017a). By fitting the present experimental data to a linear
247 function of $\Delta G_{R1}^0 = \Delta H_{R1}^0 - T\Delta S_{R1}^0$, we obtained $\Delta S_{R1}^0 = -\left(\frac{\partial \Delta G_{R1}^0}{\partial T}\right)_P = 46 \pm 3$
248 J/(mol·K). This fact suggests that the configuration entropy of Al_2O_3 bridgmanite and
249 $MgSiO_3$ corundum increase more than $MgSiO_3$ bridgmanite and Al_2O_3 corundum with
250 increasing temperatures，which is consistent with *ab initio* calculations (Panero et al.,
251 2003; Jung et al., 2010). It further means that heat capacities of two former
252 components are larger than the latter components.

253 Fig. 6 illustrates the solubility of Al_2O_3 in bridgmanite and that of $MgSiO_3$ in
254 corundum, respectively, as function of temperature up to 3000 K at 27 GPa in the
255 present and previous studies (Irifune et al., 1996; Kubo and Akaogi, 2000; Akaogi et
256 al., 2002; Liu et al., 2016, 2017a). In the present study, the Al_2O_3 solubility in
257 bridgmanite apparently increases from 24 ± 1 to 29 ± 1 mol% with increasing
258 temperature from 2750 to 3000 K. At 2850 K，bridgmanite contains 25 mol% Al_2O_3,
259 and thereby transforms into LN upon decompression. At 3000 K, we found that
260 corundum incorporates the $MgSiO_3$ component as much as 52 ± 1 mol%, which is

significantly higher than previous studies (Irifune et al., 1996; Kubo and Akaogi, 2000; Akaogi et al., 2002; Liu et al., 2016, 2017a). Dashed lines are the thermodynamic calculations using the following equation:

$$\Delta G_{R1}(P,T,X) = \Delta H_T^0 - T\Delta S_T^0 + \int_{1\ atm}^{P} \Delta V_{P,T} + 2RT\ln\frac{X_{MgSiO_3}^{Cor} X_{Al_2O_3}^{Brg}}{X_{Al_2O_3}^{Cor} X_{MgSiO_3}^{Brg}} - 2W_{Al}^{Cor}\left(1 - 2X_{Al_2O_3}^{Cor}\right) - 2W_{Al}^{Brg}\left(2X_{Al_2O_3}^{Brg} - 1\right) \quad (21)$$

where ΔH_T^0 is the enthalpy; ΔS_T^0 is the configuration entropy; T is temperature; P is the pressure; $\Delta V_{P,T}$ is the molar volume at high pressure and high temperature. Thermoelastic parameters of bridgmanite and corundum can be found in the present study for molar volume and entropy, and other parameters from Akaogi and Ito (1999) and Liu et al. (2019b). Our thermodynamics calculations show almost consistent results for the experimental data of bridgmanite. However, there exists some difference between our calculation and experimental data for corundum at temperature above 2400 K. This may be caused by poorly constrained thermoelastic parameters and large uncertainties of the interaction parameter for the Al_2O_3 corundum–$MgSiO_3$ akimotoite, which needs further studies.

4.2. Implications

It is clearly found that the Al_2O_3 solubility in bridgmanite significantly increases with increasing temperatures. Bridgmanite can contain the Al_2O_3 content up to 30 mol% at 3000 K even at a relatively low pressure of 27 GPa. This value is far beyond it in MORB compositions. From subducted basaltic slabs to the surrounding ambient lower mantle, and then to upwelling of hot plumes at the top region of the lower mantle, bridgmanite would become more aluminous due to increasing temperatures in this order, if the hot plumes have a higher Al_2O_3 content than slabs and ambient lower mantle. If the plume at the top region of the lower mantle is dominated by bridgmanite, bridgmanite with a higher Al_2O_3 content would become denser. Therefore, it may play the role of a barrier for the high temperature plumes upwelling from the lower mantle.

The LN can be used an indicator for constraining pressure and temperature conditions of shocked meteorites (e.g., Sharp et al. 1997; Ishii et al, 2017). The

present study shows a clear temperature dependence of the Al_2O_3 content in LN at the top lower mantle. Therefore, the presence of LN with aluminous enstatite compositions could be used to constrain the formation conditions of shocked meteorites. It is emphasized that, however, the presence of LN or bridgmanite with a garnet composition does not directly mean that the shock pressure was above 40 GPa (Ishii et al, 2017; Liu et al., 2019c). If the temperature had been higher than 2000 K, the shock pressure should be lower than 40 GPa, and it can be 27 GPa if the temperature were above 2800 K.

5. Conclusions

Phase relations in the system $MgSiO_3$–Al_2O_3 have been studied at temperatures of 2750–3000 K under a constant pressure of 27 GPa in a multi-anvil press. It is found that both the Al_2O_3 and $MgSiO_3$ contents, respectively, in bridgmanite and corundum have a positive temperature dependence. Bridgmanite with the Al_2O_3 content higher than 25 mol% transforms into LN upon decompression due to the incorporation of large amounts of Al. Bridgmanite and corundum, respectively, contain the Al_2O_3 and $MgSiO_3$ contents up to 30 and 52 mol.% at a temperature of 3000 K. We constrained the partial molar volumes and interaction parameters of the hypothetical end-members of Al_2O_3 bridgmanite and $MgSiO_3$ corundum. The increase in Al_2O_3 and $MgSiO_3$ contents, respectively, in bridgmanite and corundum with temperature is enhanced by their positive entropy in addition to the configuration entropy. Temperature dependence of the Al_2O_3 content in bridgmanite would help understand the dynamics of the lower mantle and constrain the pressure and temperature conditions for shocked meteorites.

Acknowledgments

We thank E. Posner, D. Krauße, R. Njul, H. Fischer, and S. Übelhack for their assistance with sample and high-pressure assembly preparation. The manuscript is greatly improved by the constructive comments of Shatskiy Anton and one anonymous reviewers and the handing editor. Z. L. was financially supported by the

Bayerisches Geoinstitut Visitor's Program and the Fundamental Research Funds for the Central Universities of Ministry of Education of China (Grant No. 45119031C037). This project has received funding from the European Research Council (ERC) under the European Union's Horizon 2020 research and innovation programme (Proposal No. 787 527) It is also supported by research grants to T. K. (BMBF: 05K13WC2, 05K16WC2; DFG: KA3434/3-1, KA3434/7-1, KA3434/8-1, KA3434/9-1) and Z. L. (the National Science Foundation of China Grant No. 41902034).

References

Akaogi, M., Ito, E., 1999. Calorimetric study on majorite–perovskite transition in the system $Mg_4Si_4O_{12}$–$Mg_3Al_2Si_3O_{12}$: transition boundaries with positive pressure–temperature slope. Phys. Earth Planet. Inter. 114, 129–140.

Akaogi, M., Tanaka, A., Ito, E., 2002. Garnet-ilmenite-perovskite transitions in the system $Mg_4Si_4O_{12}$–$Mg_3Al_2Si_3O_{12}$ at high pressures and high temperatures: phase equilibria, calorimetry and implications for mantle structure. Phys. Earth Planet. Inter. 132, 303–324.

Anderson, D.L., 1983. Chemical composition of the mantle. J. Geophys. Res. 88, 41–B52,

Brodholt, J.P., 2000. Pressure-induced changes in the compression mechanism of aluminous perovskite in the Earth's mantle. Nature 407, 620–622.

D′Amour, H., Schiferl, D., Denner, W., Schulz, H., Holzapfel, W.B., 1978. High-pressure single-crystal structure determinations for ruby up to 90 kbar using an automatic diffractometer P = 0 kbar. J. Appl. Phys. 49, 4411–4416.

Davies, P.K., Navrotsky, A., 1983. Quantitative correlations of deviations from ideality in binary and pseudo-binary solid solutions. J. Solid State Chem. 46, 1–22.

Farnetani，C.G., 1997. Excess temperature of chemical stratification mantle plumes: The role of chemical stratification across D". Geophys. Res. Lett. 24, 1583-1586.

Funamori, N., Yagi, T., Miyajima, N., Fujino, K., 1997. Transformation in garnet: from orthorhombic perovskite to $LiNbO_3$ phase on release of pressure. Science 275, 513–515.

Green, D.H., Hibberson, W.O., Jaques, A.L., 1979. Petrogenesis of mid-ocean ridge basalts. In: McElhinny, M.W. (Ed.), The Earth: Its Origin, Structure and Evolution. Academic Press, London, pp. 269–299.

Horiuchi, H., Hirano, M., Ito, E., Matsui, Y., 1982. $MgSiO_3$ (ilmenite-type): Single crystal X-ray diffraction study. Am. Mineral. 67, 788–793.

Hirose, K., Fei, Y., Yagi, T., Funakoshi, K., 2001. In situ measurements of the phase transition boundary in $Mg_3Al_2Si_3O_{12}$: implications for the nature of the seismic discontinuities in the Earth's mantle. Earth Planet. Sci. Lett. 184, 567–573.

Irifune, T., 1994. Absence of an aluminous phase in the upper part of the Earth's lower mantle. Nature 370, 131–133.

Irifune, T., Koizumi, T., Ando, J., 1996. An experimental study of the garnet-provskite transformation in the system $MgSiO_3$–$Mg_3Al_2Si_3O_{12}$. Phys. Earth Planet Inter. 96, 147–157.

Ishii, T., Shi, L., Huang, R., Tsujino, N., Druzhbin, D., Myhill, R., Li, Y., Wang, L., Yamamoto, T., Miyajima, N., Kawazoe, T., Nishiyama, N., Higo, Y., Tange, Y., Katsura, T., 2016. Generation of pressure over 40 GPa using Kawai-type multi–anvil press with tungsten carbide anvils. Rev. Sci. Instr. 87, 024501–1–024501–6.

Ishii, T., Sinmyo, R., Komabayashi, T., Boffa-Ballaran, T., Kawazoe, T., Miyajima, N., Hirose, K., Katsura, T., 2017. Synthesis and crystal structure of $LiNbO_3$-type $Mg_3Al_2Si_3O_{12}$: A possible indicator of shock conditions of meteorites. Am. Mineral. 102, 1947–1952.

Ito, E., Matsui, Y., 1978. Synthesis and crystal-chemical characterization of $MgSiO_3$ perovskite. Earth. Planet. Sci. Lett. 38, 443–450.

Jung, D.Y., Vinograd, V.L., Fabrichnaya, O.B., Oganov, A.R., Schmidt, M.W., Winkler, B., 2010. Thermodynamics of mixing in $MgSiO_3$–Al_2O_3 perovskite and ilmenite from ab initio calculations, Earth. Planet. Sci. Lett. 295, 477–48

Kubo, A., Akaogi, M., 2000. Post–garnet transitions in the system $Mg_4Si_4O_{12}$–$Mg_3Al_2Si_3O_{12}$ up to 28 GPa: phase relations of garnet, ilmenite and perovskite. Phys. Earth Planet Int. 121, 85–102.

Kudo, R., Ito, E., 1996. Melting relations in the system $Mg_4Si_4O_{12}$ (En)-$Mg_3Al_2Si_3O_{12}$ (Py) at high pressures. Phys. Earth Planet Int. 96, 159-169.

Liu, Z.D., Irifune, T., Nishi. M., Tange, Y., Arimoto, T., Shinmei, T., 2016. Phase relations in the system $MgSiO_3$– Al_2O_3 up to 52 GPa and 2000 K. Phys. Earth Planet Inter. 257, 18–27.

Liu, Z.D., Nishi. M., Ishii, T., Fei, H.Z., Miyajima, N., Boffa Ballaran, T., Ohfuji, H., Sakai, T., Wang, L., Shcheka, S., Arimoto, T., Tange, Y., Higo, Y., Irifune, T., Katsura, T., 2017a. Phase relations in the system $MgSiO_3$–Al_2O_3 up to 2300 K at lower-mantle pressures. J. Geophys. Res. 122 (10), 7775–7788

Liu, Z.D., Ishii, T., Katsura, T., 2017b. Rapid decrease of $MgAlO_{2.5}$ component in bridgmanite with pressure. Geochem. Perspect. Lett. 5, 12–18.

Liu, Z.D., Boffa Ballaran, T., Frost, D., Katsura T., 2019a. Strong correlation of oxygen vacancy in bridgmanite with Mg/Si ratios. Earth. Planet. Sci. Lett. 523, 115697

Liu, Z.D., Akaogi, M., Katsura T., 2019b. Increase of the oxygen vacancy component in bridgmanite with temperature. Earth. Planet. Sci. Lett. 505, 141–151.

Liu, Z.D., Akaogi, M., Katsura T., 2019c. A new $(Mg_{0.5}Fe^{3+}_{0.5})(Si_{0.5}Al^{3+}_{0.5})O_3$ $LiNbO_3$-type phase synthesized at lower mantle conditions. Amer Mineral 104, 1213–1216.

McCammon, C.A., 1997. Perovskite as a possible sink for ferric iron in the lower mantle. Nature 387, 694–696.

McDonough, W.F., Sun S.-s., 1995. The composition of the Earth. Chem. Geol. 120, 223–253.

Miyajima, N., Fujino, K., Funamori, N., Kondo, T., Yagi, T., 1999. Garnet-perovskite transformation under conditions of the Earth's lower mantle: an analytical transmission electron microscopy study. Phys. Earth Planet. Inter. 116, 117–131.

Navrotsky, A., Schoenitz, M., Kojitani, H., Xu, H., Zhang, J., Weidener, D.J., Jeanloz, R., 2003. Aluminum in magnesium silicate perovskite: formation, structure, and energetics of magnesium-rich defect solid solutions. J. Geophys. Res. 108, 2330.

Ringwood, A.E., 1975. Composition and Petrology of the Earth's Mantle. McGraw–Hill, New York.

Ross, N.L., Ko, J., Prewvitt, C.T., 1989. A new phase transition in $MnTiO_3$.: $LiNbO_3$-perovskite structure. Phys. Chem. Miner. 16, 621–629.

Sharp, T.G., Lingemann, C.M., Dupas, C., Stöffler, D., 1997. Natural occurrence of $MgSiO_3$-ilmenite and evidence for $MgSiO_3$-perovskite in a shocked L chondrite. Science, 277, 352–355.

Sun, S., 1982. Chemical composition and the origin of the Earth's primitive mantle. Geochim. Cosmochim. Acta 46,179–192.

Thévenin, Th., Arlès, L., Boivineau, M., Vermeulen, J.M., 1993. Thermophysical properties of rhenium. Int J Thermophys 14, 441–448.

Zhang, J., Weidner, D. J., 1999. Thermal equation of state of aluminium-enriched silicate perovskite. Science 284, 782–784.

Xu, Y., McCammon, C.A., Poe, B.T., 1998. The effect of alumina on the electrical conductivity of silicate perovskite. Science 282, 922–924.

448 **Figures caption**

449 **Figure 1.** (a) Cross section of the cell assembly. (b) Generated temperature as a
450 function of the heating powder. The inner picture is the BSE image of the recovered
451 assembly of the run IRIS624.

452 **Figure 2.** XRD profiles of the run products. The number in parenthesis represents the
453 miller induces of the first appearing phase. Question masks represent the unknown
454 peaks. Abbreviations: Brg, bridgmanite; Cor, corundum; LN, $LiNbO_3$-type phase; Sti,
455 stishovite; Re, rhenium.

456 **Figure 3.** BSE images of run products. Abbreviations: Brg, bridgmanite; Cor,
457 corundum; LN, the $LiNbO_3$-type phase; Sti, stishovite; Re, rhenium.

458 **Figure 4.** Molar volume of bridgmanite and corundum in the system $MgSiO_3$–Al_2O_3
459 in previous studies.

460 **Figure 5.** Gibbs free energy of reaction (1) as a function of temperature. The data at
461 temperatures of 1700–2500 K are from Liu et al. (2016, 2017a).

462 **Figure 6.** The Al_2O_3 and $MgSiO_3$ contents, respectively, in bridgmanite and
463 corundum as a function of temperature. Dashed lines are thermodynamics calculation
464 results.

Table 1. Starting materials, experimental conditions, and runs products

Run No.	Start Comp.	P (27 GPa) / T (K) / t (minut	Phases
IRIS624	$En_{75}Cor_{25}$	2750/10	LN+Cor + trace Brg+Sti
IRIS635	$En_{75}Cor_{25}$	2850/3	LN + Cor + Re
	$En_{65}Cor_{35}$		LN + Cor + Re
IRIS627	$En_{65}Cor_{35}$	3000/3	LN + Cor + Re

Abbreviations: Brg, bridgmanite; Cor, corundum; LN, LiNbO3-type phase; Sti, stishovite.

Table 2. Chemical compositions of the bridgmanite and LN-type phases.

Run. No.	IRIS624	IRIS635		IRIS627	
Comp.	$En_{75}Cor_{25}$	$En_{75}Cor_{25}$	$En_{65}Cor_{35}$	$En_{65}Cor_{35}$	
Phases	Brg/LN (n = 12)	LN (n = 11)	LN (n = 10)	LN (n =12)	Cor (n = 8)
MgO	30.58 (68)	30.26 (22)	29.85 (70)	16.47 (49)	28.19 (45)	20.62(83)
Al_2O_3	23.77 (54)	25.42 (20)	26.50 (55)	58.30 (72)	28.96 (81)	49.22 (119)
SiO_2	45.34 (91)	44.73 (45)	43.87 (43)	24.70 (93)	42.60 (42)	31.09 (75)
Total	99.70 (119)	97.82 (58)	100.21 (96)	99.48 (76)	99.74 (41)	100.93 (68)
Mg	0.767 (11)	0.754 (5)	0.745 (13)	0.416 (11)	0.707 (11)	0.244 (14)
Al	0.471 (13)	0.501 (3)	0.523 (12)	1.165 (21)	0.574 (16)	0.718 (13)
Si	0.763 (9)	0.747 (4)	0.735 (4)	0.419 (13)	0.716 (7)	0.277 (12)
Σcation	2.001 (5)	2.002 (3)	2.003 (4)	1.999 (4)	1.997 (2)	1.998 (5)
Component (mol%)						
$MgSiO_3$	76 (1)	75 (0)	74 (1)	42 (1)	71 (1)	52 (1)
Al_2O_3	24 (1)	25 (0)	26 (1)	58 (1)	29 (1)	48 (1)
Total	100	100	100	100	100	100

Oxide analyses are reported in wt.%. n: number of analysis points. The oxygen number of Brg and LN is normalized to 3. Number in parentheses represents standard deviation for the last digit (s). Abbreviations: Brg, bridgmanite; LN, $LiNbO_3$-type

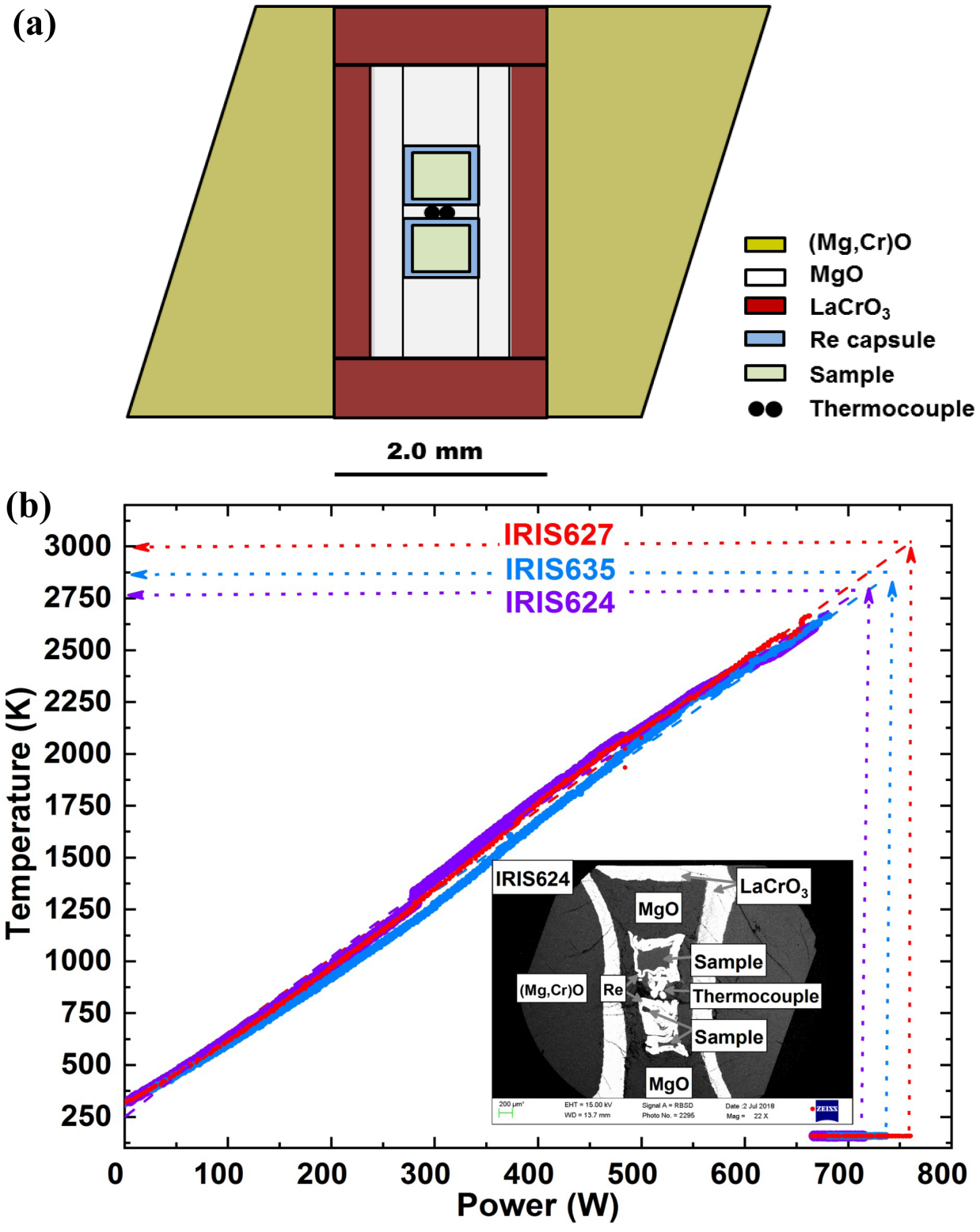
(a)
(Mg,Cr)O
MgO
LaCrO3
Re capsule
Sample
Thermocouple
2.0 mm
(b)
IRIS627
IRIS635
IRIS624
Temperature (K)
Power (W)
IRIS624
LaCrO3
MgO
Sample
(Mg,Cr)O
Re
Thermocouple
Sample
MgO

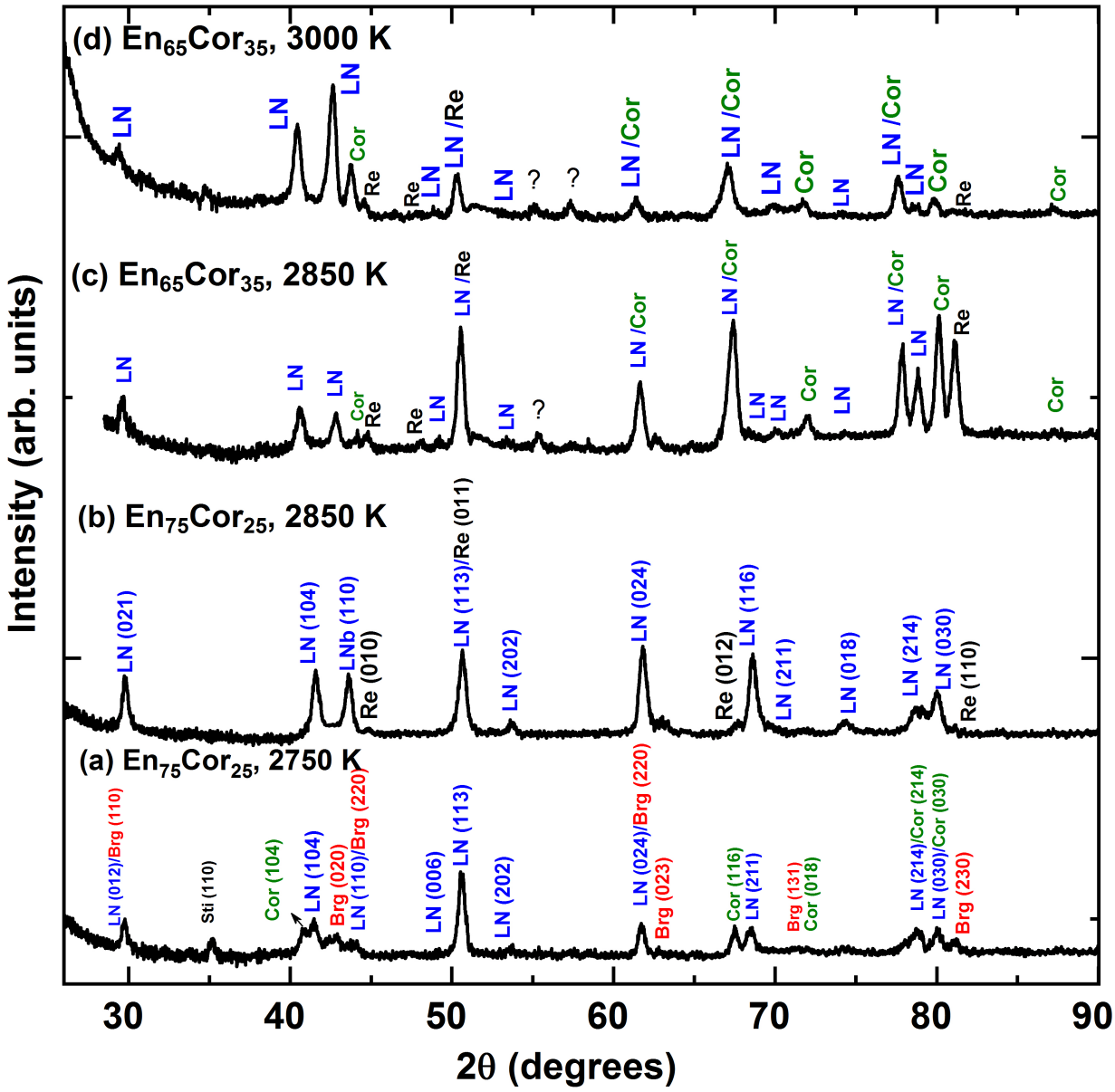
(d) En65Cor35, 3000 K
(c) En65Cor35, 2850 K
(b) En75Cor25, 2850 K
(a) En75Cor25, 2750 K
Intensity (arb. units)
2θ (degrees)
30
40
50
60
70
80
90
LN (021)
LN (104)
LNb (110)
Re (010)
LN (113)/Re (011)
LN (202)
LN (024)
Re (012)
LN (116)
LN (211)
LN (018)
LN (214)
LN (030)
Re (110)
LN (012)/Brg (110)
Sti (110)
Cor (104)
LN (104)
Brg (020)
LN (110)/Brg (220)
LN (006)
LN (113)
LN (202)
LN (024)/Brg (220)
Brg (023)
Cor (116)
LN (211)
Brg (131)
Cor (018)
LN (214)/Cor (214)
LN (030)/Cor (030)
Brg (230)

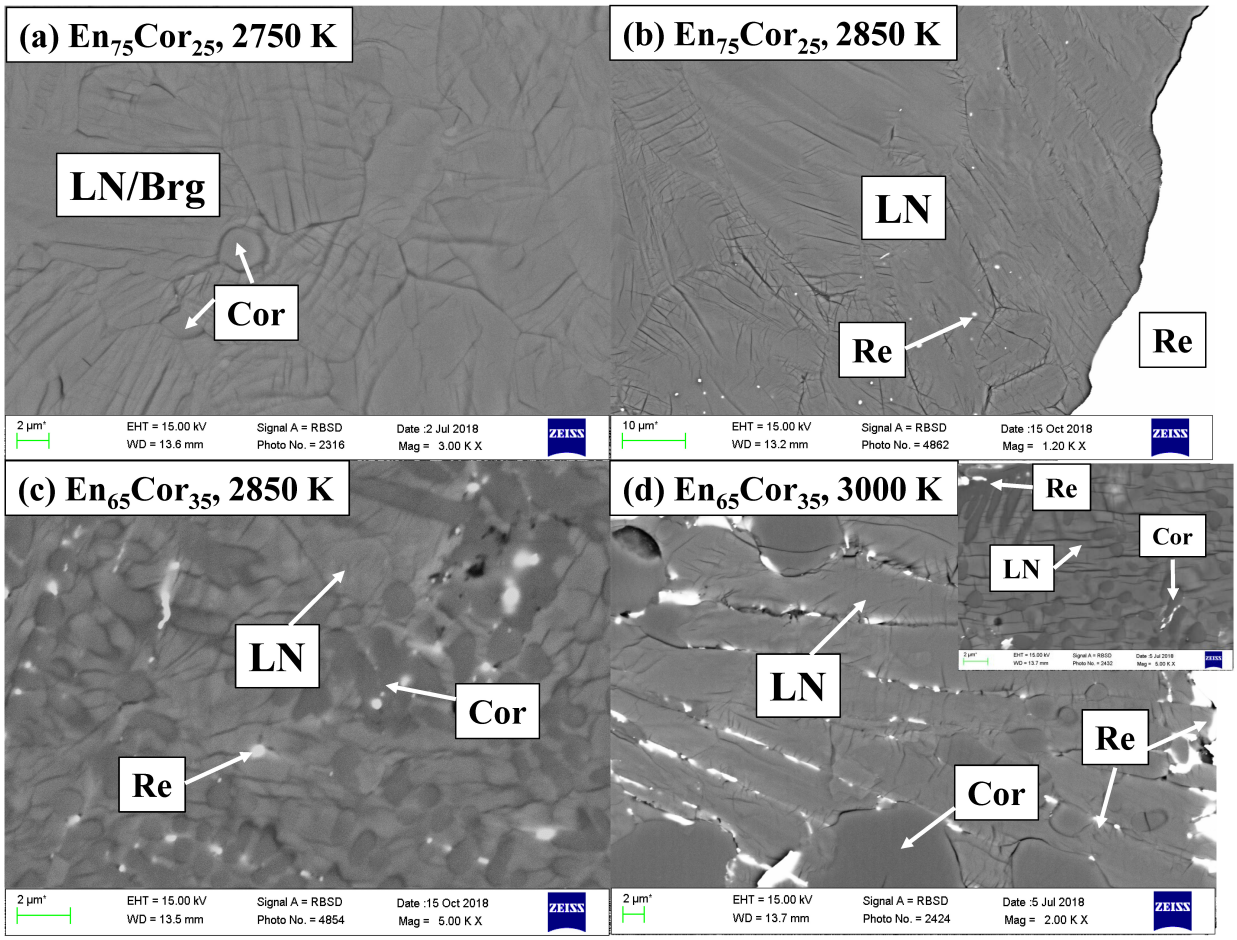
(a) En75Cor25, 2750 K
LN/Brg
Cor
2 µm*
EHT = 15.00 kV
WD = 13.6 mm
Signal A = RBSD
Photo No. = 2316
Date :2 Jul 2018
Mag = 3.00 K X
ZEISS
(b) En75Cor25, 2850 K
LN
Re
Re
10 µm*
EHT = 15.00 kV
WD = 13.2 mm
Signal A = RBSD
Photo No. = 4862
Date :15 Oct 2018
Mag = 1.20 K X
ZEISS
(c) En65Cor35, 2850 K
LN
Cor
Re
2 µm*
EHT = 15.00 kV
WD = 13.5 mm
Signal A = RBSD
Photo No. = 4854
Date :15 Oct 2018
Mag = 5.00 K X
ZEISS
(d) En65Cor35, 3000 K
Re
LN
Cor
LN
Re
Cor
2 µm*
EHT = 15.00 kV
WD = 13.7 mm
Signal A = RBSD
Photo No. = 2424
Date :5 Jul 2018
Mag = 2.00 K X
ZEISS

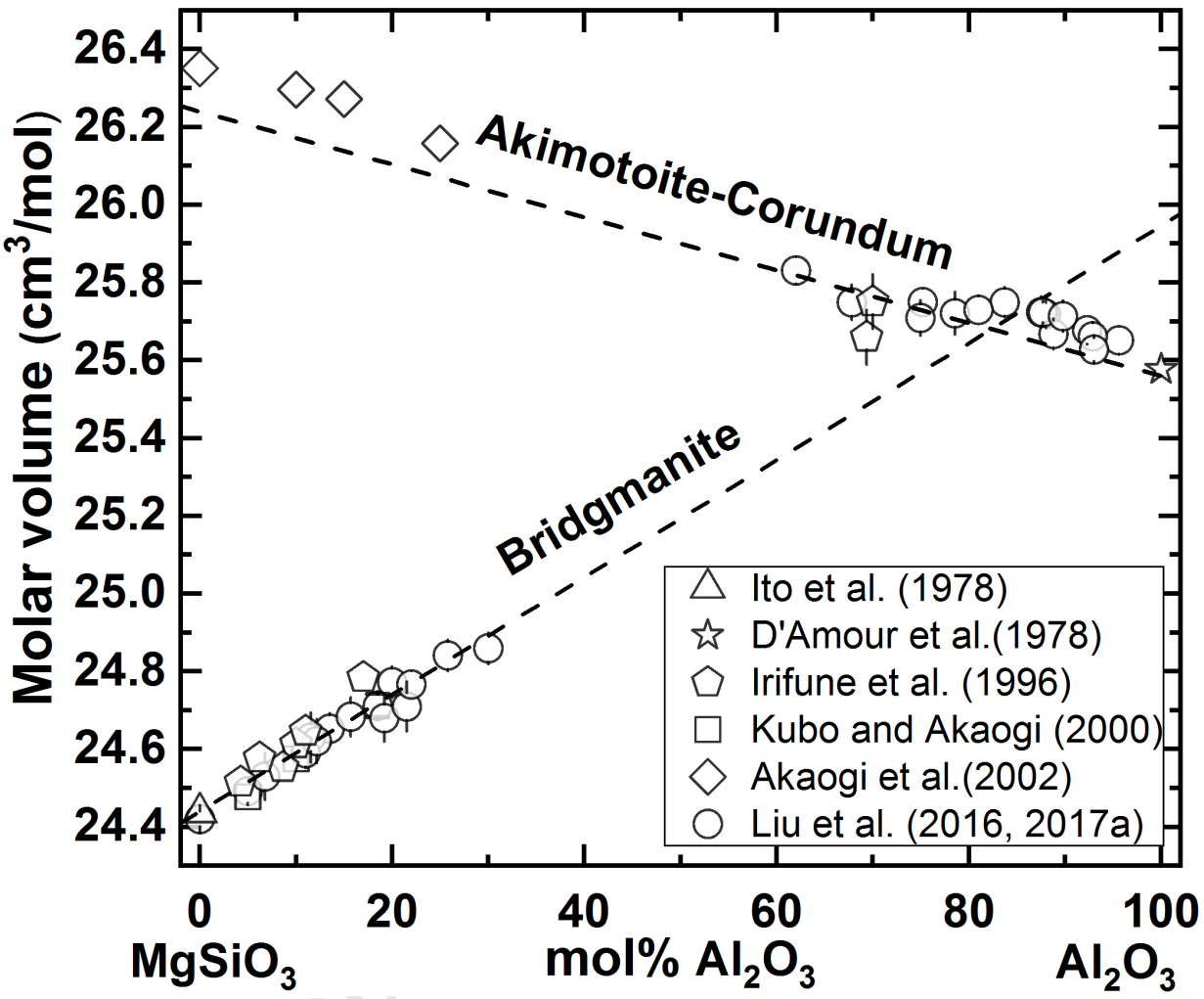
Molar volume (cm3/mol)
26.4
26.2
26.0
25.8
25.6
25.4
25.2
25.0
24.8
24.6
24.4
Akimotoite-Corundum
Bridgmanite
Ito et al. (1978)
D'Amour et al.(1978)
Irifune et al. (1996)
Kubo and Akaogi (2000)
Akaogi et al.(2002)
Liu et al. (2016, 2017a)
0
20
40
60
80
100
MgSiO3
mol% Al2O3
Al2O3

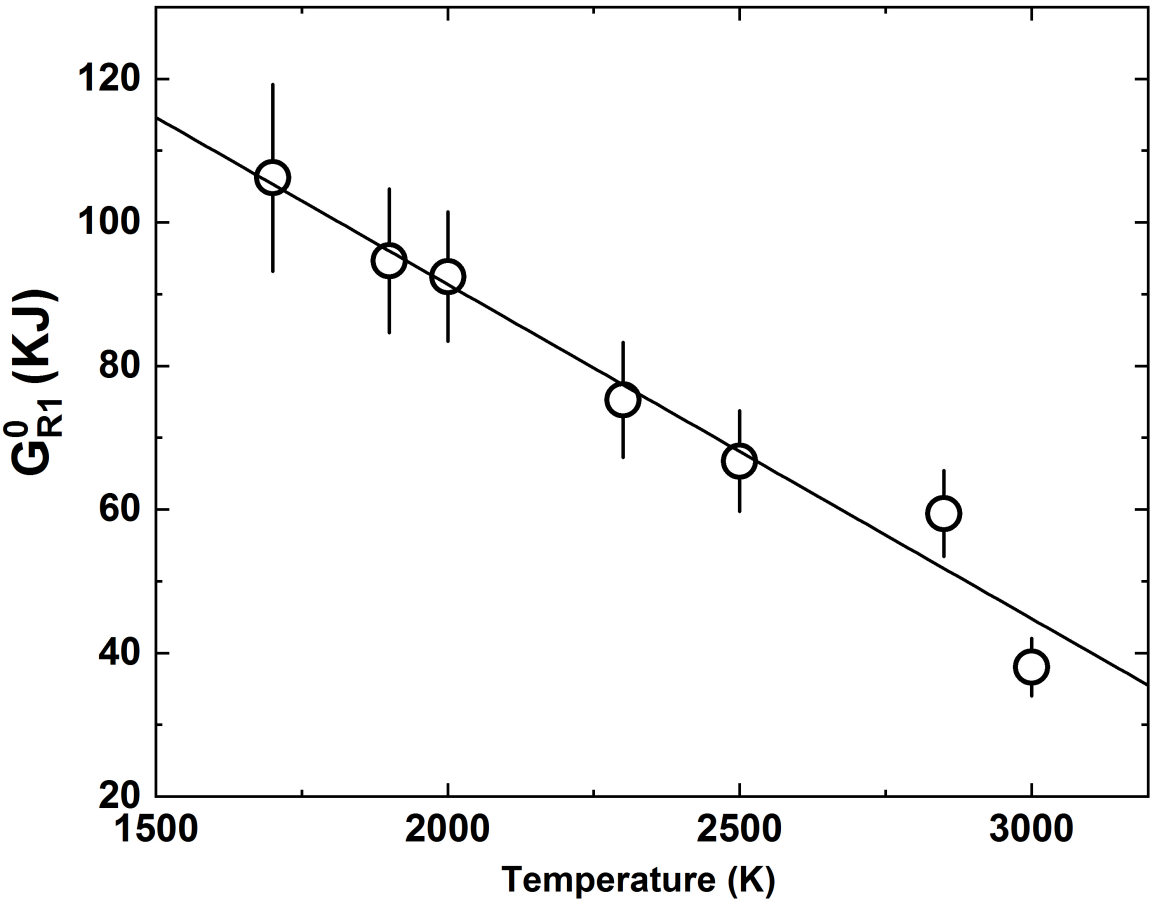

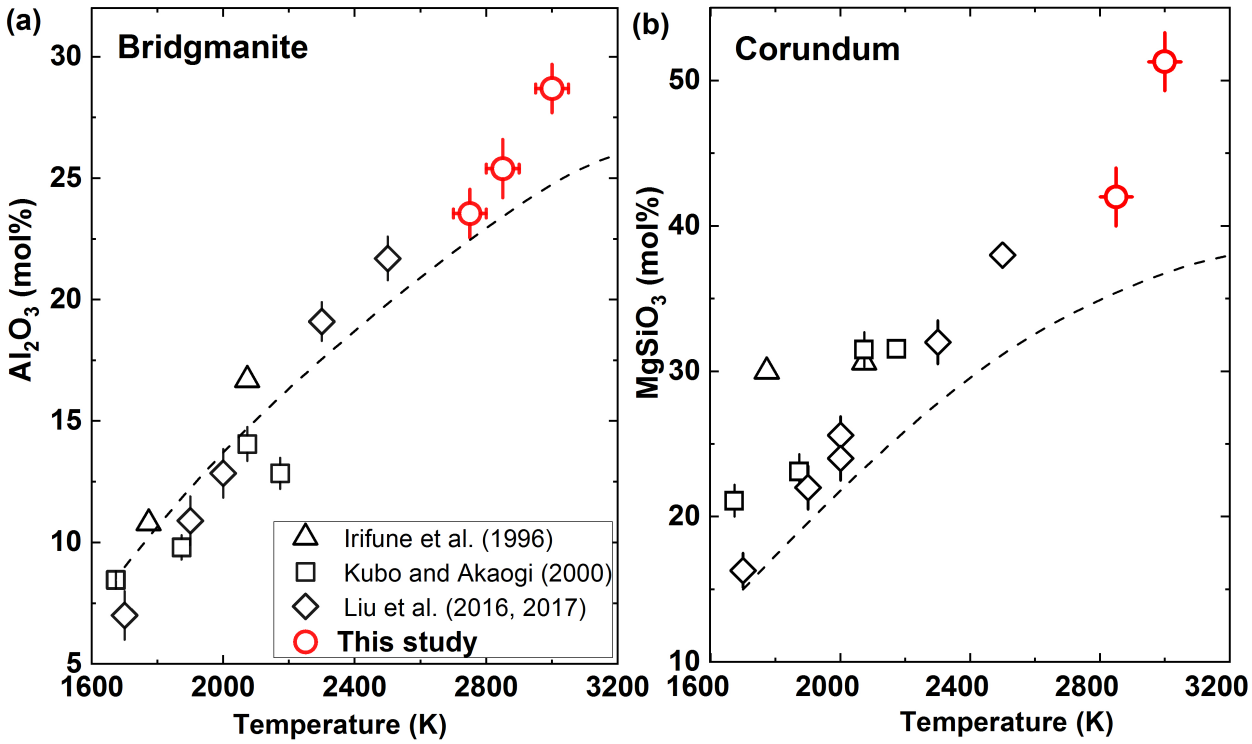

Highlights of "**Aluminum solubility in bridgmanite up to 3000 K at the top lower mantle**"

Zhaodong Liu[1, 2 *], Ran Liu[2],Yuchen Shang[2], Fangrui Shen[2], Luyao Chen[2], Xuyuan, Hou[2], Mingguang Yao[2], Tian Cui[2], Bingbing Liu[2], Tomoo Katsura[1,3]

[1]Bayerisches Geoinstitut, University of Bayreuth, Bayreuth 95440, Germany.

[2] State Key Laboratory of Superhard Materials, Jilin University, Changchun 130012, China

[3]Center for High Pressure Science and Technology Advanced Research, Beijing, 100094, P.R. China

* Corresponding author: Zhaodong Liu (liu_zhaodong@jlu.edu.cn)

Highlights:

1. Phase relations in the system $MgSiO_3$-Al_2O_3 were determined up to 3000 K at 27 GPa.
2. Bridgmanite can contain 30 mol% Al_2O_3 at 27 GPa and 3000 K.
3. The solubility of Al_2O_3 in bridgmanite and that $MgSiO_3$ in corundum increase with temperatures.
4. We constrain the molar volume and non-ideality of Al_2O_3 bridgmanite and $MgSiO_3$ corundum.
5. Temperature dependence of Al_2O_3 solubility in bridgmanite may explain the dynamics of the top lower mantle.

Declaration of interests

The authors declare that they have no known competing financial interests or personal relationships that could have appeared to influence the work reported in this paper.